NASA/TM—2000-209645

Inception of Snapover and Gas Induced Glow Discharges

J.T. Galofaro
Glenn Research Center, Cleveland, Ohio

B.V. Vayner
Ohio Aerospace Institute, Brook Park, Ohio

W.A. Degroot
Dynacs Engineering Company, Inc., Brook Park, Ohio

D.C. Ferguson
Glenn Research Center, Cleveland, Ohio

C.D. Thomson, J.R. Dennison, and R.E. Davies
Utah State University, Logan, Utah

January 2000

The NASA STI Program Office . . . in Profile

Since its founding, NASA has been dedicated to the advancement of aeronautics and space science. The NASA Scientific and Technical Information (STI) Program Office plays a key part in helping NASA maintain this important role.

The NASA STI Program Office is operated by Langley Research Center, the Lead Center for NASA's scientific and technical information. The NASA STI Program Office provides access to the NASA STI Database, the largest collection of aeronautical and space science STI in the world. The Program Office is also NASA's institutional mechanism for disseminating the results of its research and development activities. These results are published by NASA in the NASA STI Report Series, which includes the following report types:

- TECHNICAL PUBLICATION. Reports of completed research or a major significant phase of research that present the results of NASA programs and include extensive data or theoretical analysis. Includes compilations of significant scientific and technical data and information deemed to be of continuing reference value. NASA's counterpart of peer-reviewed formal professional papers but has less stringent limitations on manuscript length and extent of graphic presentations.

- TECHNICAL MEMORANDUM. Scientific and technical findings that are preliminary or of specialized interest, e.g., quick release reports, working papers, and bibliographies that contain minimal annotation. Does not contain extensive analysis.

- CONTRACTOR REPORT. Scientific and technical findings by NASA-sponsored contractors and grantees.

- CONFERENCE PUBLICATION. Collected papers from scientific and technical conferences, symposia, seminars, or other meetings sponsored or cosponsored by NASA.

- SPECIAL PUBLICATION. Scientific, technical, or historical information from NASA programs, projects, and missions, often concerned with subjects having substantial public interest.

- TECHNICAL TRANSLATION. English-language translations of foreign scientific and technical material pertinent to NASA's mission.

Specialized services that complement the STI Program Office's diverse offerings include creating custom thesauri, building customized data bases, organizing and publishing research results . . . even providing videos.

For more information about the NASA STI Program Office, see the following:

- Access the NASA STI Program Home Page at ***http://www.sti.nasa.gov***

- E-mail your question via the Internet to help@sti.nasa.gov

- Fax your question to the NASA Access Help Desk at (301) 621-0134

- Telephone the NASA Access Help Desk at (301) 621-0390

- Write to:
  NASA Access Help Desk
  NASA Center for AeroSpace Information
  7121 Standard Drive
  Hanover, MD 21076

NASA/TM—2000-209645

Inception of Snapover and Gas Induced Glow Discharges

J.T. Galofaro
Glenn Research Center, Cleveland, Ohio

B.V. Vayner
Ohio Aerospace Institute, Brook Park, Ohio

W.A. Degroot
Dynacs Engineering Company, Inc., Brook Park, Ohio

D.C. Ferguson
Glenn Research Center, Cleveland, Ohio

C.D. Thomson, J.R. Dennison, and R.E. Davies
Utah State University, Logan, Utah

National Aeronautics and
Space Administration

Glenn Research Center

January 2000

Available from

NASA Center for Aerospace Information
7121 Standard Drive
Hanover, MD 21076
Price Code: A03

National Technical Information Service
5285 Port Royal Road
Springfield, VA 22100
Price Code: A03

INCEPTION OF SNAPOVER AND GAS INDUCED GLOW DISCHARGES

J.T. Galofaro
National Aeronautics and Space Administration
Glenn Research Center
Cleveland, Ohio

B.V. Vayner
Ohio Aerospace Institute
Brook Park, Ohio

W.A. Degroot
Dynacs Engineering Company, Inc.
Brook Park, Ohio

D.C. Ferguson
National Aeronautics and Space Administration
Glenn Research Center
Cleveland, Ohio

C.D. Thomson, J.R. Dennison, and R.E. Davies
Utah State University
Logan, Utah

Abstract

Ground based experiments of the snapover phenomenon were conducted in the large vertical simulation chamber at the Glenn Research Center (GRC) Plasma Interaction Facility (PIF). Two Penning sources provided both argon and xenon plasmas for the experiments. The sources were used to simulate a variety of ionospheric densities pertaining to a spacecraft in a Low Earth Orbital (LEO) environment[1–4]. Secondary electron emission is believed responsible for dielectric surface charging, and all subsequent snapover phenomena observed[2,5]. Voltage sweeps of conductor potentials versus collected current were recorded in order to examine the specific charging history of each sample. The average time constant for sample charging was estimated between 25 and 50 seconds for all samples. It appears that current drops off by approximately a factor of 3 over the charging time of the sample. All samples charged in the forward and reverse bias directions, demonstrated hysteresis. Current jumps were only observed in the forward or positive swept voltage direction. There is large dispersion in the critical snapover potential when repeating sweeps on any one sample. The current ratio for the first snapover region jumps between 2 and 4.6 times, with a standard deviation less than 1.6. Two of the samples showed even larger current ratios. It is believed the second large snapover region is due to sample outgassing. Under certain preset conditions, namely at the higher neutral gas background pressures, a perceptible blue-green glow was observed around the conductor. The glow is believed to be a result of secondary electrons undergoing collisions with an expelled tenuous cloud of gas, that is outgassed from the sample. Spectroscopic measurements of the glow discharge were made in an attempt to identify specific lines contributing to the observed glow.

I. Introduction

Snapover describes a sudden and rather dramatic change in the current collection regime in and around positively biased conductors that are surrounded by a dielectric[6–9]. Specifically there is a dramatic transition from the normal current collection regime to a regime exhibiting high current collection. Such current jumps can only be brought about by successively biasing a conductor to increasing positive bias potentials, in a time interval, that is comparable to the charging time of the dielectric. Dielectric surface charging is brought about by secondary electron emission[5,6,9]. A small percentage of primary electrons, having the proper energy and

trajectory, will be focused onto the surface of the dielectric by the E-field. The focusing effects are typically limited to a small area of the dielectric, extending over a small radial distance ≈ 1–2 cm from the outward edge of the conductor/ dielectric interface. As primary electrons strike the dielectric one or more secondaries can be liberated. As the sheath area grows, the surface of the dielectric quickly charges to a positive potential. Secondary electrons, suffering collisions with the outgassed species, are responsible for excitation and the resulting glow. Ferguson et al. reported snapover-induced glow in ground tests using argon, xenon and neon plasmas[10].

The increased complexity of modern spacecraft is fueling the requirement for higher voltage power system designs. Others have previously demonstrated that the high voltage spacecraft systems are capable of undergoing significant physical interactions with the plasma environment[11,12]. The 160 V solar array, designed to provide power, for the International Space Station represents a prime example[9,11]. A solar array is most vulnerable to snapover at the instant it comes out of eclipse into full sunlight. The solar array voltage will quickly ramp up to full operating potential. With current spacecraft solar array voltages, and the large number of conductor and dielectric surfaces in close proximity, there is increased danger of snapover induced electrical discharges disrupting spacecraft power systems[13–15].

II. Experimental Test Apparatus

All snapover electrical and optical experiments were run in a 1.8m diameter by 3m high vertical vacuum chamber. Two penning type plasma sources provided plasma for the experiments. The penning sources use a hot filament to ionize either argon or xenon neutral gas which is slowly bleed into the chamber through a controllable leak valve. An ionization gauge was used to measure chamber pressure as gas was added to the chamber via the leak valve. Electron plasma number densities for the experiments ranged from 2×10^5 to 4.0×10^6 electrons/cm^3 and electron temperatures were on the order of 1–3.5 eV.

A sample table was constructed of fiberglass and was mounted in a vertical position in the vacuum chamber. Twenty sample coupons of various types (see figure 1) were then affixed to the sample table so that they could be clearly observed through an optical viewing port on the chamber wall. The sample coupons consisted of a central conductor of a specific metal type (copper or aluminum) and geometry (cylinder or hemispherical), imbedded in a 0.635cm thick by 10.16cm long by 10.16cm wide square of dielectric material. Cylinder diameters for both copper and aluminum conductors are given on the sample key at the bottom of figure 1. All conductors, with the exception of the hemisphere, were mounted flush with the top surface of the dielectric. Sample coupons were then prepared with a dielectric composed of Kapton, Teflon, or silicon dioxide (Sio2).

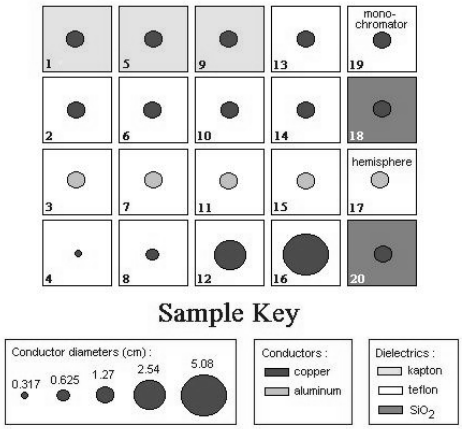

Figure 1.—Sample coupon testbed used in snapover experiments.

Electrical connections were made to the backside of the conductor and each sample coupon was connected to a separate electrical feed through. The exposed back of each conductor was then insulated with a silicone type adhesive. All sample coupons were electrically floated in the vacuum chamber. A programmable source and measure unit allowed a single conductor sample to be swept with respect to the chamber ground, while simultaneously measuring the current at each bias voltage step. In this way it was possible to obtain a volt/ampere curve for each sample.

For the snapover-induced glow experiments a single 1.27cm aluminum-Teflon coupon test sample was mounted on a separate insulated stand. The coupon was positioned so that it could be clearly seen through a 15.24cm diameter quartz window mounted on the vacuum chamber wall. Insulated electrical connections were then made between the sample and the electrical feedthrough port.

A 10cm diameter double convex lens with a focal distance of 24cm was mounted inside the chamber, between the sample and quartz optical viewing port. The position between the lens and the sample was adjusted at 85cm, so that the nearly parallel light rays from the sample would be focussed just outside the optical view port. The position of the spectrometer was then adjusted so that the focal point of the lens would fall exactly on the 50μ wide entrance slit. A black cylindrical light shield tube was constructed around the lens and the optical view port to shield stray light generated by the plasma sources.

This spectrometer employs a Czerny-Turner optical design (see figure 2(a)). Light passing through the entrance slit undergoes 3 specular reflections before passing through the exit assembly. The focal length of the instrument is 156mm. The grating has 1200 groves per mm, and was cut with a blaze angle centered on 300nm peak intensity. The usable wavelength range for this particular grating is 190nm to 600nm. The manufacturer claims a resolution of 1nm for the instrument.

Light passing from the exit assembly is detected by a charge-coupled device (CCD). The detector/ controller is plumed with 2 lines, a chilled water to cool the detector head and a dry gaseous nitrogen line to prevent against condensation. Figure 2(b) shows a block diagram of the apparatus used in obtaining the optical spectra. Information that is gathered by the controller/detector is passed to a computer via a parallel interface and card. Appropriate software, provided by the manufacturer, was used to capture and store information displayed on the computer screen.

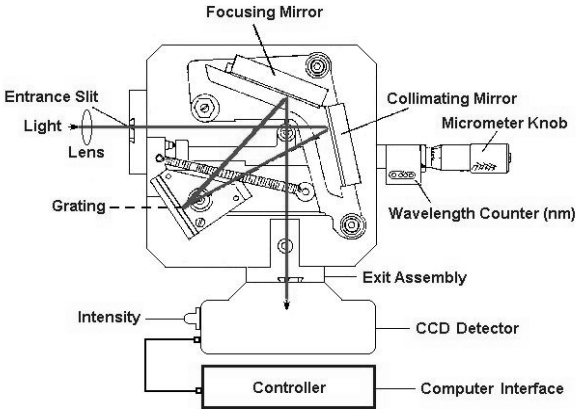

Figure 2(a).—Spectrometer setup used in analyzing snapover-induced glow.

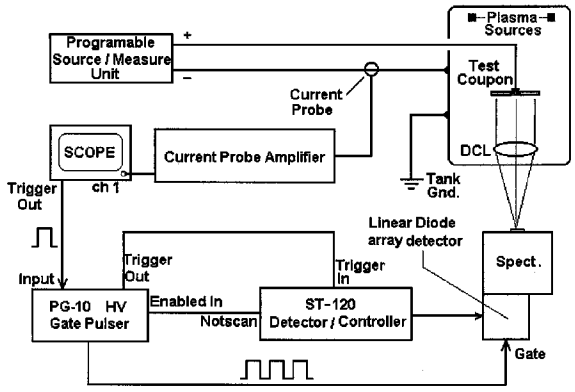

Figure 2(b).—Applied voltage bias between coupon and tank ground causes gaseous discharge. Current pulse detected by current probe triggers channel 1 of the scope. Output trigger from scope causes HV Gate Pulser to open Gate and obtain spectra.

III. Experimental Snapover Results

The first series of tests were run to determine the time constant of the sample. The sample was biased from V=0 volts potential and then immediately to some large positive potential. Figures 3(a) and 3(b) show the current to the sample recorded at various time intervals. These hand plots show the charging constant, τ to be roughly between 25s and 50s. Note that the current drops by a factor of 3 over the time constant in figures 3(a) and 3(b). The floating potential, V_f was measured at 5.5 volts in these tests.

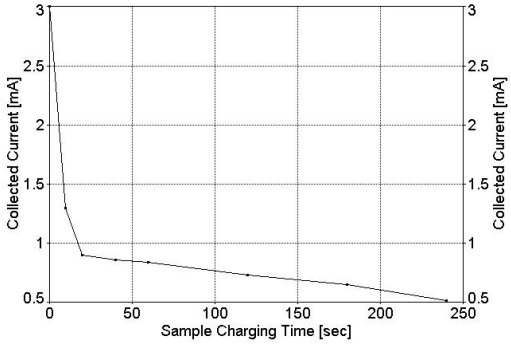

Figure 3(a).—Sample curve for sample biased from 0 to +600 volts.

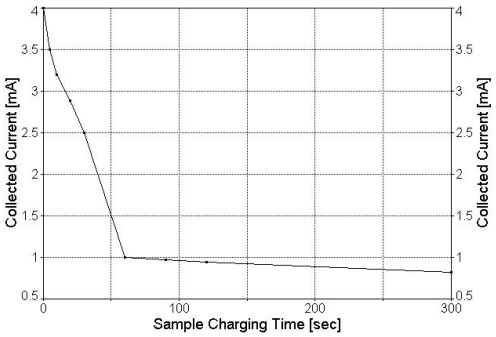

Figure 3(b). —Sample curve for sample biased from 0 to +700 volts.

The next series of tests involved snapover. The 1.27cm copper-Teflon sample was biased up in an argon plasma. The neutral gas background pressure, $P_o = 7.3\times10^{-5}$ Torr, the plasma number density, $N_e = 2\times10^{5}$ cm^{-3} and the electron temperature, $T_e = 3.5$eV. A sweep was made by biasing the conductor from –100V to +400V in 10V steps with a step time 0.5s at each bias voltage. There are several irregularities in the forward biased voltage-current trace (figure 3(a)). The observed hook at the first large current jump at 200V is believed to be due to outgassing of the sample (more will be said about outgassing later). A sweep in the reverse bias direction (figure 3(b)) does not show any peculiarities. Note the hysteresis between the forward and reverse bias traces in figures 4(a) and 4(b).

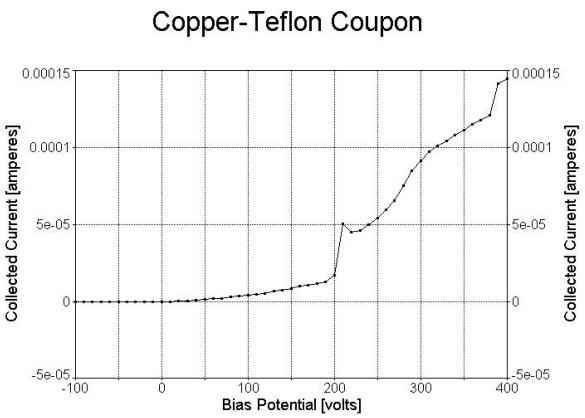

Figure 4(a).—Forward bias sweep showing current jumps at 200V, 300V, and 380V.

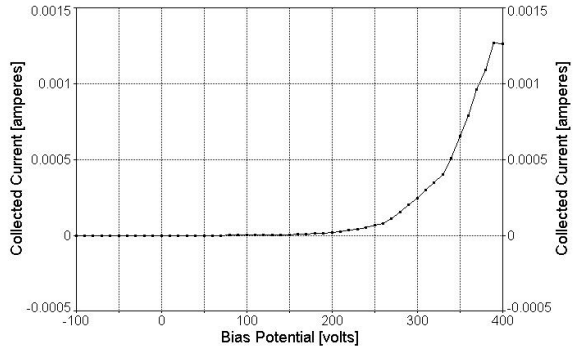

Figure 4(b).—Reverse bias sweep shows a smooth curve sweep typical of a conductor.

In order to verify the effect of current jumping two more sweeps have been obtained from the same 1.27cm copper-Teflon coupon (sample 19). Figure 5(a) demonstrates the single large current jump at 250V is thought to be a result of outgassing. The "hook" in the curve at 250V is characteristic of a gas discharge at high voltage. Figure 5(b) appears to demonstrate a shifting of the critical voltage to a higher snapover potential. If this effect is do to outgassing we should observe the disappearance of the large current jump at 250V in the second sweep of sample 19. Also note the absence of the hook in figure 5(b) appears to demonstrate that the sample is well outgassed.

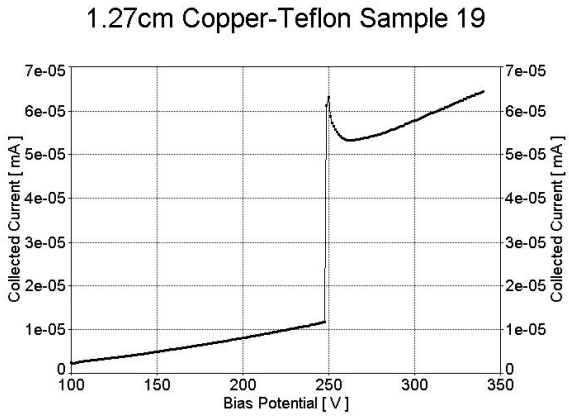

Figure 5(a).—Current-voltage sweep at 10:30 a.m., 10V steps and 0.5s per step.

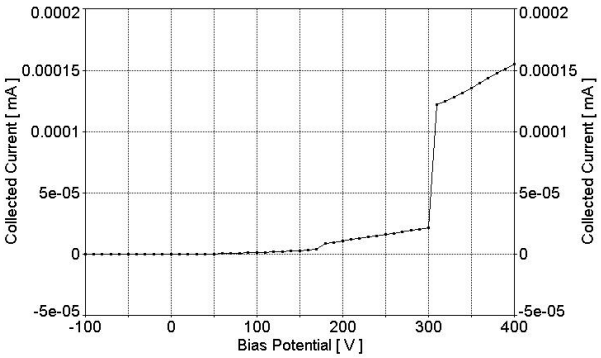

Figure 5(b).—Current-voltage sweep at 2:30 p.m., 10V steps and 0.5s per step. The critical voltage shifted at 300V.

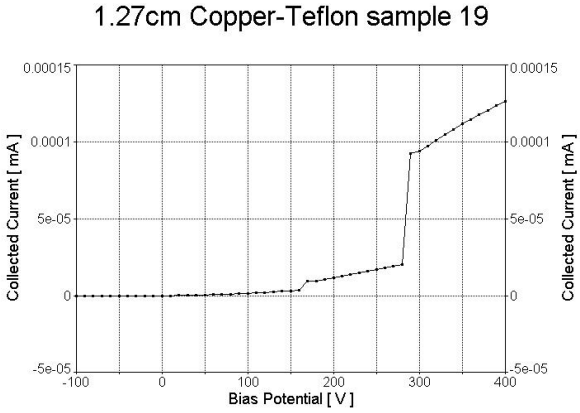

Figure 5(c).—Critical voltage decreases from 300V to 275V but the effect is repeatable.

In order to verify the effect of current jumping two more sweeps have been obtained from the same 1.27cm copper-Teflon coupon (sample 19). Figure 5(a) demonstrates the single large current jump at 250V is thought to be a result of outgassing. The "hook" in the curve at 250V is characteristic of a gas discharge at high voltage. Figure 5(b) appears to demonstrate a shifting of the critical voltage to a higher snapover potential. If this effect is do to outgassing we should observe the disappearance of the large current jump at 250V in the second sweep of sample 19. Also note the absence of the hook in figure 5(b) appears to demonstrate that the sample is well outgassed.

The sample coupons have been sitting in the vacuum chamber for some 48 hours. Assuming the effect of current jumping is caused by outgassing one should observe a rise in the critical voltage for snapover on coupon sample 19. In reality the critical voltage was measured at 200V for the virgin sample. After sitting in vacuum for a few hours the critical voltage increased to about 300V (figure 5(b)). The critical voltage then decreases to 275V after sitting in the vacuum chamber for another 20 hours (figure 5(c)).

It was decided to keep the sample coupons in the vacuum for a much greater length of time (3 more days) before continuing the tests on the other samples. For the proceeding tests $P_o = 7.3\times10^{-5}$ Torr (consisting of argon gas neutrals), $N_e = 3.3\times10^{+5}$ cm^{-3}, and $T_e = 2.2$ eV for the experiments. In order to obtain good statistical results a minimum of 10 sweeps were performed on each sample coupon. The results of these results are summarized in Table 1.

Table 1.—Summary of snapover results for various sample coupons.

Coupon Type	Sample Size[cm]	Sample #	Snapover Voltage [V]	Standard Deviation	Current Ratio	Standard Deviation	Increase (in Area)	Standard Deviation
Copper-Teflon	1.270	1	279	25	3.18	0.87	2.88	1.27
Copper-Teflon	1.270	2	289	47	4.60	1.23	2.34	0.52
Aluminum-Teflon	1.270	3	243	6	4.50	0.17	3.40	0.70
Copper-Teflon	0.317	4	230	23	47.0	16.0	43.8	13.6
Copper-Teflon	0.625	8	316	51	29.0	21.0	21.7	16.0
Copper-Teflon	2.540	12	198	6	3.25	1.00	2.18	0.63
Copper-Teflon	5.080	16	211	14	1.96	0.33	1.91	0.33
Aluminum-Teflon	0.625	17	268	12.6	4.70	1.60	2.97	0.95
Copper-SiO2 (Glass)	0.625	18	232.5	4.64	4.90	0.87	15.9	1.46

The snapover results reported in table 1 need further explanation. Three standard measurements are shown in table 1: Snapover Voltage, Current Ratio, and Increase in area. These tabular values represent the mean value for 10 independent measurements of the particular parameter in of interest for a given sample. To the right of each standard measurement is a field containing the standard deviation or spread of values about the mean determination.

The snapover voltage refers to the inception voltage at the first current jump (first snapover region). The current ratio is a scalar factor referring to the magnitude of the collected current. This magnitude is computed by dividing the current maximum by the current minimum in the first snapover region. Finally the increase in area is a fictitious term referring to the effective increase in sheath collecting area. The increase in collected area is governed by sheath size; orbit limited current collection, secondary yield, E-field, and surface conductivity. The increase in area is computed from the ratio of the slopes of the current-voltage curve directly before and after the first jump in current at the inception voltage.

Statistical data for snapover inception voltage appears to be widely scattered for all samples. It is interesting to note that sample 16, the largest conductor of all samples tested, showed a second large current jump in all ten sweeps. Samples 4 and 8 showed large dispersion in their standard deviations for all three standard measurements. The reason for the large dispersions is believed to be due to contamination of dielectric surfaces. After completing the various snapover tests on the samples and after completing the initial glow observations, it was discovered that yellow stains were found around all electrodes of the biased samples. An inspection of these stains, performed by three pairs of experienced eyes, have confirmed that the contamination is diffusion pump oil possibly due to a valve failure experienced earlier. None of the unbiased virgin samples inspected showed stains of any kind. The samples were cleaned with a methyl alcohol wash and returned to the vacuum chamber after drying.

IV. Optical Results

In order to verify the hypothesis of a gas discharge at high voltage, our eyes and a color video camcorder has been employed. Previous attempts at GRC to see snapover induced glow with the human eye proved allusive, even at voltages as high as 600V. Such gaseous discharges were strongly felt to result from Paschen breakdown. If vacuum arc ignition is indeed the cause of such gaseous discharges then the glow would be strongly dependent on two parameters: pressure and voltage[16]. Since changes in voltage alone failed to produce the glow, it was decided that the other parameter pressure needed to be adjusted.

An argon plasma was established in the vacuum chamber with a much greater neutral gas background pressure (P_o = 3×10^{-4} Torr) then previously used. Next a previously unbiased virgin sample (sample 11) was slowly swept from +100V to +600V in 5V steps. The voltage was applied over a time of 500ms at each step. As the sample was swept, observations of the sample were made with the unaided eye through the vacuum chamber's optical view port. An 8cm diameter blue-green glowing ring of gas was detected around the electrode at approximately 515V. The glow lasted about 10s before extinguishing. A second attempt at biasing sample 11 failed to produce the glow. The absence of the glow appears to confirm the initial suspicion of sample outgassing. It is suggested here that sample outgassing, due to gas and/or water vapor trapped between the conductor-dielectric interface, is responsible. In fact a blue color is often seen in plasmas where water vapor is present.

Moving to a new virgin sample (sample 2) a camcorder was set up to record the glow. The sample was biased positive and the glow (see figure 6) was recorded. Figure 7 shows the voltage-current sweep for the glow recorded shown in figure 6.

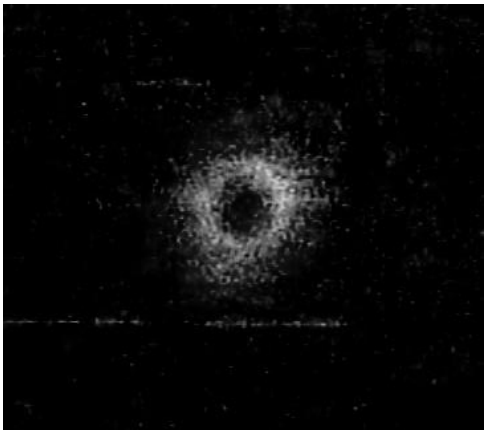

Figure 6.—Example of snapover induced glow discharge.

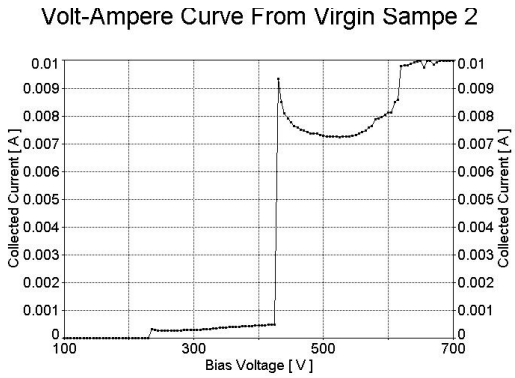

Figure 7.—Gaseous discharge begins at about 430V potential.

The finial series experiments were performed in an attempt to obtain a glow discharge spectrum. Sample 19 was cleaned and mounted in the tank facing the quartz optical view port. An argon lamp was mounted in mounted in front of the sample. The distance of the culminating lens was adjusted to a sharp focus on the slit. For calibration purposes, an argon spectrum was obtained by rotating the grating and obtaining a calibration spectrum for argon at the following central wavelengths, (λ): λ = 385nm, λ = 400nm, λ = 420nm, λ = 435nm, λ = 450nm, and λ = 470nm. A sample argon spectrum with the spectrometer adjusted on the 420nm line is shown in figure 8. The overall estimate of error for this conversion process is 1nm (10 angstroms) [17].

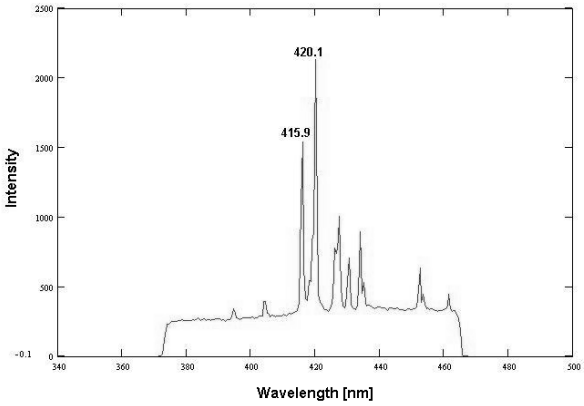

Figure 8.—Sample argon calibration spectrum with two of the most intense lines labeled.

In reality the output obtained from the instrument software is given in terms of pixels (scalar) and intensity (relative units). Conversion from pixels to wavelength, λ, is obtained from the following equation:

$$\lambda(p) \cong 420.1 - k(p - b(\lambda_c))$$

where p = pixel number, k = 0.125 nm per pixel, λ_c = 385nm, 400nm, 420nm, 435nm, 450nm, and 470nm (central wavelength adjustment set on the spectrometer), b(385) = 246.5, b(400) = 370.5, b(420) = 534.5, b(435) = 654.5 and b(450) = 774.5. Exact details of the conversion process as well as estimate of errors can be found in Vayner et. al. (reference 17).

Having completed the calibration of the spectrometer the argon lamp was removed and the vacuum chamber was pumped down. The tank pressure with the argon plasma sources operating was $P_o = 3.2\times10^{-4}$ Torr.

In practice the spectrometer is adjusted to a specific central wavelength, λc and a background trace was acquired. The plasma source hot filaments produce a modest wide band background signal centered at about 550nm. This background needs to be subtracted from every glow spectrum acquired. The background also needs to be newly acquired ever time the spectrometer central wavelength is re-adjusted. A minimum of two glow spectra was acquired at each λ_c specified in the argon calibration spectrum. Figure 9 shows a typical glow spectrum obtained in an argon plasma.

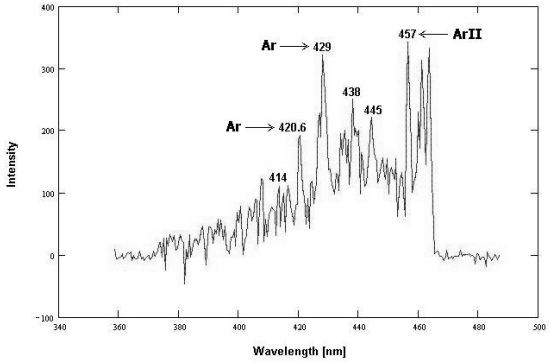

Figure 9.—Glow spectrum in argon plasma. Spectrometer set for λ_c = 420nm.

It should be noted that a shift to higher frequencies in λ_c translates to a shift to the right (shift to higher λ's) in the acquired spectrum.

The finial series of measurements were aimed at obtaining a glow discharge spectrum in the presence of a xenon plasma. The base operating pressure with the plasma sources on was $P_o = 2\times10^{-4}$ Torr. Once again, a minimum of two glow discharge spectra was acquired at each λ_c specified in the argon calibration spectrum. Background traces obtained at each shift in λ_c were subtracted from the corresponding glow discharge spectrum. Figure 10 demonstrates a typical glow spectrum obtained in a xenon plasma.

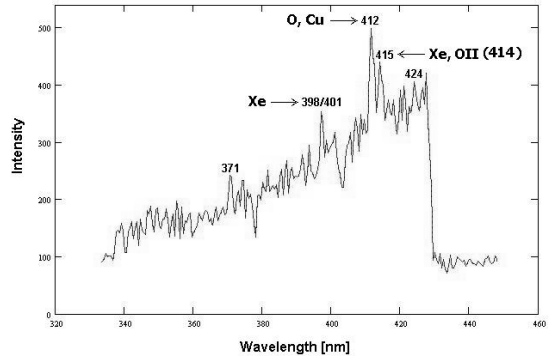

Figure 10.—Glow spectrum in a xenon plasma. Spectrometer set λ_c = 385nm.

A direct comparison of spectrum measurements performed for different λc in both argon and xenon plasmas are made. These comparisons were used to determine the most reliable lines and common lines in the glow discharge spectrum.

For argon plasmas the following lines were identified: 403, 410, 414, 418, 420.6, 425, 428.6, 438, 444, 456, and 461/63. In xenon plasmas the following lines were also identified: 371, 398/401, 412/415, 419, 422/24, and 454. The MIT Tables[18] show the most intensive lines for xenon occur at 419nm, 414nm and 398nm. Lines at 414nm in argon and the 412/415 lines for xenon may belong to some other species in the glow spectrum. No lines for xenon were found at 401nm. Lines for oxygen at 412nm, for copper at 412nm and for OII at 414nm were found. There is a strong line for xenon at 454nm. No suitable species was found at 456nm. There are however lines at 457.7nm for OI and a line at 457.9nm for ArII.

V. Conclusion

Snapover and related solar array interactions with the space plasma environment are issues of great importance. An understanding of the snapover phenomenon is therefore valuable to solar array system design and survivability. Modern high power solar arrays are currently being used in a number of spacecraft. A number of these spacecraft are experiencing problems that can be related to snapover. Large planar arrays, incorporating insulators adjacent to exposed conductors in the space plasma, can effectively collect current as if they were conductors. Such enhanced plasma current collection was detected in the laboratory on the PASP Plus flight arrays[4]. The reason for this type of current collection behavior is due to enhanced surface conductivity resulting from secondary electron emission. The present experiments were conducted to study the effects of enhanced current collection in the laboratory for a number of different dielectrics and conductor types. Snapover induced glow discharges, a related phenomenon, was also studied at pressure ranges between 10^{-4} and 10^{-5} Torr. Although these pressures are much higher than what might ordinarily be found in low Earth orbit, they are more typical of what might be found during brief periods of spacecraft thruster firings. Spectroscopic analysis of the glow discharge has allowed several lines contributing to the glow to be isolated, but not the contributing species. It is hoped the present study is beneficial to the scientific community.

VI. References

1. Staskus, J.V., "Electron Beam Charging of Space Shuttle Protection System Tiles", Spacecraft Environmental Interactions Technology, NASA CP–2359, 1983, pp. 91–102.

2. Stevens, N.J. and Domitz, S., "Interaction Between Spacecraft and the Charged Particle Environment", Spacecraft Charging Technology, NASA CP–2071, 1978, pp. 268–294.

3. Ferguson, D.C., Snyder, D.B. and Carruth, R, "Findings of the Joint Workshop on Evaluation of Impacts of Space Station Freedom Ground Configurations", NASA TM–103717, 1990.

4. Ferguson, D.C., "Comparison of Electron Current Collection by Space Station Solar arrays as Measured by SAMPIE and PASPlus", Photovoltaic Array Space Power Plus Diagnostics (PASP Plus) Experiment Final Report, PL–TR–97–1013, March 1997, pp. 7-1.

5. Katz, I. Et, Mandell, M.J., and Jongeward, G.A., "A Three dimensional Dynamic Study of Electrostatic Charging in Materials. NASA CR–135256, 1977.

6. Galofaro, J.T. "Comparison of Currents Predicted by NASCAP/LEO Model Simulations with Elementary Langmuir Type Bare Probe Models for an Insulated Cable Containing a Pinhole", NASA TM–102486, July 1990, pp. 3–5.

7. Cole, R.K., Ogawa, H.S., and Sellen, J.M., "Operation of Solar Cell Arrays in Dilute Streaming Plasmas", TRW–09357–6006–R000, NASA Contract NAS3–10612, NASA CR–72376, 1968.

8. Kennerude, K.L., "High Voltage Solar Array Experiments", NASA CR–121280, 1974.

9. Grier, N.T., and McKinzie, D.J., Jr., "Current Drainage to a High Voltage Probe in a Dilute Plasma", NASA TM–X–67890, 1971.

10. Ferguson, D., Hillard, G., Snyder, D., and Grier, N., "The Inception of Snapover on Arrays: A Visualization Technique", 36th AIAA–98–1045, Aerospace Sciences Meeting and Exhibit, Reno, NV, January 12–15, 1998, pp. 1–8.

11. Vaughn, J.A., Carruth, Jr., M.R., Zkatz, I., Mandell, M.J., and Jongeward, G.A., "Electrical Breakdown Currents on Large Spacecraft in a Low Earth Orbit," Journal of Spacecraft and Rockets, vol. 31, no. 1, 1994, pp. 54–59.

12. McCoy, J.E., and Konradi, A., "Sheath Effects Observed on a 100 Meter High Voltage Panel in Simulated Low Earth Orbit," Proceedings of Spacecraft Charging Technology 1978, NASA CP–2071, October—November 1978, pp. 201–210.

13. Davis, V. and Gardner, B., "Parasitic Current Collection by Solar Cells in LEO," AIAA Paper 95–0594, 1995.

14. Ferguson, D.C., "Preliminary Results from the Flight of the Solar Array Module Plasma Interactions Experiment (SAMPIE)," Proceedings of the XIII Space Photovoltaic and Research and Technology Conference, NASA CP–3278, 1994.

15. Hillard, G.P., "Plasma Chamber Testing of Advanced Photovoltaic Solar Array Coupons," Journal of Spacecraft and Rockets, vol. 31, no. 3, 1993, pp. 530–532.

16. Boxman, R.L., Sanders, D..M., Martin, P. J. and Lafferty, J.M., "Handbook of Vacuum Arc Science and Technology," Fundamentals and Applications, Noyes Publications, New Jersey, USA, pp. 61–62.

17. Vayner, B., Galofaro, J., Ferguson, D., and Degroot, W., "A Comprehensive Study of Dielectric-Conductor Junction in Low Density Plasmas", Proc. 38th AIAA Aerospace Sciences Meeting and Exhibit", 2000–0871, January 10–13, Reno, NV.

18. Harrison, G.R., "Massachusetts Institute of Technology Wavelength Tables" with Intensities in Arc, Spark, or Discharge Tube of more than 100,000 Spectrum Lines Between 10,000 A. and 2000 A., M.I.T. Press, Cambridge, Massachusetts, and London, England, 1969, pp. 117–207.

REPORT DOCUMENTATION PAGE

Form Approved
OMB No. 0704-0188

1. AGENCY USE ONLY (*Leave blank*)	2. REPORT DATE	3. REPORT TYPE AND DATES COVERED
	January 2000	Technical Memorandum

4. TITLE AND SUBTITLE

Inception of Snapover and Gas Induced Glow Discharges

5. FUNDING NUMBERS

WU–632–1A–1L–00

6. AUTHOR(S)

J.T. Galofaro, B.V. Vayner, W.A. Degroot, D.C. Ferguson, C.D. Thomson, J.R. Dennison, and R.E. Davies

7. PERFORMING ORGANIZATION NAME(S) AND ADDRESS(ES)

National Aeronautics and Space Administration
John H. Glenn Research Center at Lewis Field
Cleveland, Ohio 44135–3191

8. PERFORMING ORGANIZATION REPORT NUMBER

E–11991

9. SPONSORING/MONITORING AGENCY NAME(S) AND ADDRESS(ES)

National Aeronautics and Space Administration
Washington, DC 20546–0001

10. SPONSORING/MONITORING AGENCY REPORT NUMBER

NASA TM—2000-209645

11. SUPPLEMENTARY NOTES

J.T. Galofaro and D.C. Ferguson, NASA Glenn Research Center; B.V. Vayner, Ohio Aerospace Institute, 22800 Cedar Point Road, Brook Park, Ohio 44142; W.A. Degroot, Dynacs Engineering Company, Inc., 2001 Aerospace Parkway, Brook Park, Ohio 44142; C.D. Thomson, J.R. Dennison, and R.E. Davies, Utah State University, Logan, Utah 84322-0001. Responsible person, J.T. Galofaro, organization code 5410, (216) 433–2294.

12a. DISTRIBUTION/AVAILABILITY STATEMENT

Unclassified - Unlimited
Subject Categories: 18, 46 and 74 Distribution: Nonstandard

This publication is available from the NASA Center for AeroSpace Information, (301) 621–0390.

12b. DISTRIBUTION CODE

13. ABSTRACT ***(Maximum 200 words)***

Ground based experiments of the snapover phenomenon were conducted in the large vertical simulation chamber at the Glenn Research Center (GRC) Plasma Interaction Facility (PIF). Two Penning sources provided both argon and xenon plasmas for the experiments. The sources were used to simulate a variety of ionospheric densities pertaining to a spacecraft in a Low Earth Orbital (LEO) environment. Secondary electron emission is believed responsible for dielectric surface charging, and all subsequent snapover phenomena observed. Voltage sweeps of conductor potentials versus collected current were recorded in order to examine the specific charging history of each sample. The average time constant for sample charging was estimated between 25 and 50 seconds for all samples. It appears that current drops off by approximately a factor of 3 over the charging time of the sample. All samples charged in the forward and reverse bias directions, demonstrated hysteresis. Current jumps were only observed in the forward or positive swept voltage direction. There is large dispersion in the critical snapover potential when repeating sweeps on any one sample. The current ratio for the first snapover region jumps between 2 and 4.6 times, with a standard deviation less than 1.6. Two of the samples showed even larger current ratios. It is believed the second large snapover region is due to sample outgassing. Under certain preset conditions, namely at the higher neutral gas background pressures, a perceptible blue-green glow was observed around the conductor. The glow is believed to be a result of secondary electrons undergoing collisions with an expelled tenuous cloud of gas, that is outgassed from the sample. Spectroscopic measurements of the glow discharge were made in an attempt to identify specific lines contributing to the observed glow.

14. SUBJECT TERMS

Snapover; Gaseous discharges; Anodized coatings; Spectroscopy; Low density plasmas

15. NUMBER OF PAGES

14

16. PRICE CODE

A03

17. SECURITY CLASSIFICATION OF REPORT	18. SECURITY CLASSIFICATION OF THIS PAGE	19. SECURITY CLASSIFICATION OF ABSTRACT	20. LIMITATION OF ABSTRACT
Unclassified	Unclassified	Unclassified	